

# Direct determination of absolute molecular stereochemistry in gas phase by Coulomb explosion imaging

Martin Pitzer<sup>1</sup>, Maksim Kunitski<sup>1</sup>, Allan S. Johnson<sup>1,2</sup>, Till Jahnke<sup>1</sup>, Hendrik Sann<sup>1</sup>, Felix Sturm<sup>1</sup>, Lothar Ph. H. Schmidt<sup>1</sup>, Horst Schmidt-Böcking<sup>1</sup>, Reinhard Dörner<sup>1</sup>, Jürgen Stohner<sup>3</sup>, Julia Kiedrowski<sup>4</sup>, Michael Reggelin<sup>4</sup>, Sebastian Marquardt<sup>4</sup>, Alexander Schießer<sup>4</sup>, Robert Berger<sup>4\*</sup>, Markus S. Schöffler<sup>1\*</sup>

<sup>1</sup>Institute for Nuclear Physics,

Johann Wolfgang Goethe-University Frankfurt,

Max-von-Laue-Str. 1, 60438 Frankfurt, Germany

<sup>2</sup>University of Ottawa, Ottawa, ON, Canada K1N 6N5

<sup>3</sup>Institute of Chemistry and Biological Chemistry,

Zurich University of Applied Sciences, Campus Reidbach,

Einsiedlerstr. 31, 8820 Wädenswil, Switzerland

<sup>4</sup>Clemens-Schöpf Institute,

TU Darmstadt,

Petersenstr. 22, 64287 Darmstadt, Germany

\*To whom correspondence should be addressed;

E-mail: schoeffler@atom.uni-frankfurt.de,

robert.berger@tu-darmstadt.de

**Bijvoet's method, which utilizes anomalous X-ray diffraction or dispersion, is the standard means of direct determination of the absolute (stereochemical) configuration of molecules, but it requires crystalline samples and often proves challenging in structures exclusively comprising light atoms. Herein**

**we demonstrate a mass spectrometry approach that directly images the absolute configuration of individual molecules in gas phase by cold target recoil ion momentum spectroscopy (COLTRIMS) following laser ionization-induced Coulomb explosion. The technique is applied to the prototypical chiral molecule bromochlorofluoromethane (CHBrClF) and the isotopically chiral methane derivative bromodichloromethane (CHBr<sup>37</sup>Cl<sup>35</sup>Cl).**

A molecule that cannot be superposed with its mirror image by pure translation and rotation is termed chiral, with the non-identical mirror-images denoted as enantiomers. If it were not for the predicted tiny contributions due to parity-violating weak interactions (*I*), which are currently searched for in high-precision molecular physics experiments on chiral molecules (2, 3), the energy levels of both enantiomers would be equal. They can be distinguished by their interaction with other chiral objects, for instance left- or right-handed molecules and left- or right-handed circularly polarized photons. The latter type of interaction led Louis Pasteur more than one and a half centuries ago to the first discovery of molecular chirality by observing optical rotation in aqueous solutions of manually separated enantiomorphous crystals from double salts of tartaric acid (4). Van't Hoff (5) and Le Bel (6) independently ascribed Pasteur's observation to an underlying three-dimensional structure of molecules, which can result in two non-identical mirror image structures.

Enantiomers can be distinguished comparatively easily by their chiroptical signals, such as optical rotation, that are of (nearly, due to parity-violation) equal magnitude but opposite sign. This is manifested by the frequently used phenomenological (+/−) terminology. The microscopic structure, on the other hand, is classified with the systematic *R/S* or *P/M* stereodescriptors (7). Assigning the absolute (stereochemical) configuration, however, i.e. establishing which of the two possible mirror-image spatial structural models gives rise to optical rotation with positive or negative sign, still poses a challenge.

The standard approach to directly determine absolute configuration is Bijvoet's method (8) of 1951, but after the technique of Coulomb explosion imaging (CEI) had been established (9), it was in 2001 pointed out as a potential means to determine the handedness of chiral molecules (10). Before 1951 chemical or biochemical conversions were used that relate compounds of unknown configuration to others with known configuration, a method which is still applied today. For this purpose Fischer (11) had arbitrarily assigned a given three dimensional structural model (denoted as the D-form) of saccharic acid to the compound that is weakly (+) rotating in aqueous solution and its mirror image (L-form) to the (−) rotating counterpart. Subsequently (see also Ref. (12) for the historical development), catalogues of the D and L series could be established, the components of which were chemically related either directly to D or L saccharic acid or to other chiral molecules already filed in the catalogue. Bijvoet finally confirmed (8) Fischer's arbitrary choice by studying the sodium rubidium double salt of tartaric acid with anomalous X-ray diffraction. Heavy elemental scatterers induce a pronounced phase and intensity shift when irradiated with X-rays near their absorption edge, which allows the determination of absolute configuration. While typically quite conclusive, Bijvoet's method is limited by requiring crystalline samples. A promising new approach using X-ray diffraction has recently been presented by Inokuma et al. (13). They inserted a chiral liquid sample into a crystalline host framework containing heavy atoms. Due to the interaction, the framework's symmetry changed to a chiral spacegroup, thus allowing the application of anomalous X-ray diffraction. Nonetheless, conventional crystallographic challenges and flaws, such as misassigned atoms, symmetry problems and guest disorder, persist and thus require support from mass spectrometry or nuclear magnetic resonance (13).

The lack of versatile direct approaches has led to the active exploration of indirect physico-chemical approaches based on optical rotation and circular dichroism. Indirect methods rely on quantum chemical calculations or empirical rules to interpret the experimental data. Al-

ternatively, liquid chromatography with an enantioselective stationary phase is a wide-spread method for chiral discrimination. Its drawback for assignment lies in the need for a suitable analogue with known stereochemical configuration. Recent activities focus on nuclear magnetic resonance (NMR) spectroscopy, either by seeking to turn NMR directly into a chiroptical method (14) or by exploring possibilities to use residual dipolar couplings in chiral non-racemic alignment media (15). Also photo-electron circular dichroism has received renewed interest (16) and promising three-wave mixing strategies to obtain chiroptical signals in microwave spectroscopy have been reported recently (17).

Herein we focus on direct determination of absolute configuration in the gas phase by a molecular imaging technique that displays the three-dimensional structure of individual chiral molecules on a detector and thereby permits assignment of absolute configuration on a single-molecule basis. Kitamura et al. used a similar approach, but with highly charged argon atoms from an ion source as ionizing agents, to detect dynamical chirality in perdeuterated methane (10) and pointed out the possibility of detecting molecular handedness. In 2008, Gagnon et al. employed a related variant to study the structure of achiral dichloromethane ( $\text{CH}_2\text{Cl}_2$ ) (18) by CEI. For the direct assignment of the absolute configuration high count rates for 4-fold or higher fragmentation coincidence events are required. The laser systems commercially available back in 2008 were unable to produce such rates. To overcome apparatus limitations for stereochemical assignments, we combine in this work latest high-power femtosecond lasers of 10 to 100 times higher repetition rates (100 kHz) with improved fast hexanode delay-line detectors to surmount otherwise prohibitively long data acquisition time. In addition, we employ high-performance data recording techniques together with an off-line analysis protocol to cope with the increasing complexity emerging for polyatomic molecules (19). These improvements allow to utilize CEI to determine the absolute configuration of the prototypical chiral compound bromochlorofluoromethane ( $\text{CHBrClF}$ ) and for isotopically chiral methane

derivatives in natural abundance such as  $\text{CHBr}^{37}\text{Cl}^{35}\text{Cl}$ .

$\text{CHBrCl}_2$  is commercially available and was used without further purification as impurities are easily discarded in the analysis step of coincidence experiments. Racemic  $\text{CHBrClF}$  was synthesized as described in Ref. (20) by reacting  $\text{CHBr}_2\text{Cl}$  with  $\text{HgF}_2$ . The spectrometer system employed was described in detail in Ref. (21). For the present study the setup was augmented by an assembly of cold traps to recycle the volatile sample compounds.

The approach for direct determination of absolute configuration employs the well established COLd Target Recoil Ion Momentum Spectroscopy (COLTRIMS) as sketched in Fig. S1 in the Supplementary Material. A supersonic gas jet of chiral molecules ( $y$ -axis in the laboratory system) crosses either a high-power femtosecond laser (laboratory  $x$ -axis) to induce multiple ionization and resulting the Coulomb explosion or a synchrotron radiation beam (results not reported here) or an ion beam. Charged fragments are projected by a static electric field along the laboratory  $z$ -axis onto a position and time sensitive multichannel plate detector (MCP) with hexagonal delayline readout (22) where all fragments are detected in coincidence (see Fig. S2). From the impact position on the detector ( $x, y$ ), the known distance between ionization zone and MCP, as well as the measured time-of-flight  $t$ , the velocities of all cations (formed in coincidence) can be derived. By assigning masses and charges to the various fragments, corresponding linear momenta of all detected particles can be obtained. In molecular multiple ionization and fragmentation the momenta of photons and electrons are usually negligible compared to the momenta of the Coulomb exploding ionic fragments. Hence, in a cold molecular beam, the sum of the ion momentum vectors has to be close to zero due to momentum conservation. The mass assignment can therefore be confirmed by checking this computed total momentum of all ions. Assignment of absolute configuration is in principle already possible, once four charged fragments (e.g.  $\text{Br}^+$ ,  $\text{Cl}^+$ ,  $\text{F}^+$  and  $\text{CH}^+$  for  $\text{CHBrClF}$ ) are detected in coincidence. Signatures of those break-ups could be found in the data and used for assign-

ment (results not reported here). Herein, however, we focus on the complete fragmentation into five singly charged ions because analysis and interpretation are more straightforward. Additionally the background can be suppressed quite efficiently. Mass resolution in COLTRIMS is sufficient to distinguish various isotopes of bromine and chlorine in natural abundance, thereby even allowing stereochemical characterization of isotopically chiral molecules.

Further details of the measurement method can be located in the supporting material (SM) (23).

Fig. 1 shows the sum of all ion momenta in the case where five fragments of CHBrClF are measured in coincidence. The peak at zero total momentum shows events with the correct mass assignment  $^{79}\text{Br}^+$ ,  $^{35}\text{Cl}^+$ ,  $^{19}\text{F}^+$ ,  $^{12}\text{C}^+$  and  $^1\text{H}^+$ . These events were used for the determination of the absolute configuration. The peaks at lower momentum in  $z$ -direction are contributions from other isotopologues.

Fig. 2 demonstrates the capability to distinguish enantiomers in our racemic sample. For this purpose, an angle  $\theta$  is defined, indicating if the momenta of bromine, chlorine and fluorine form a right-handed or a left-handed coordinate system. As distinct peaks are obtained in the histogram, almost all events can be assigned clearly to one enantiomer or the other. This shows the robustness of our method against the laser pulse length: Being about 40 fs long, our pulses are not short enough to consider the hydrogen frozen during multiple ionization. The clear separation of enantiomers in the histogram indicates, however, that the motion of hydrogen during the laser pulse does not alter bond angles to an extent that would prevent identification of enantiomers. These results also show that reconstruction of the exact geometric structure is not necessary for the determination of absolute configuration. Classical molecular dynamics simulations confirm that the enantiomers are mapped unambiguously onto their momentum space analogues that are presented here.

Fig. 3 overlays measured linear momenta on a rigid structural model of neutral CHBrClF,

with the linear momentum of carbon fixed along the  $x$ -axis, the momentum sum of chlorine and bromine defining the  $x$ - $y$ -plane and all other linear momenta being oriented relative to these. For better visibility, momenta are normalized with respect to the carbon momentum. The momentum of hydrogen, being very small due to the low mass, is expanded by a factor of two in this figure. It is evident that the configuration of the two enantiomers is directly imaged on the detector. As a racemic mixture of CHBrClF was employed, an equal ratio for  $S$ - and  $R$ -configuration was obtained within the statistical uncertainty (329 and 302 events for  $S$  and  $R$ , respectively, with  $|\cos(\theta)| > 0.6$  in each case). At first sight one might be surprised that the carbon ion is detected in the same direction as the proton. This is due to the fact that the position of the center of mass is conserved and thus  $H^+$  and  $C^+$ , as the lightest two ions of the system, are repelled from the slowly moving heavier ions, as has been confirmed with the help of molecular dynamics simulations.

For CHBrClF the direct assignment of absolute configuration works unequivocally in the majority of fivefold coincidence events due to the comparatively large mass difference between the ions. The situation is considerably more challenging for the case of isotopically chiral systems. In the case of CHBrCl<sub>2</sub> (see Fig. 4), not all five-fold fragmentation events allow an unambiguous assignment of the isotope masses to each fragment and hence no determination of absolute configuration is possible for such events. However, a subset of events that permit a conclusive assignment can be selected by a procedure detailed in the SM (Figs. S3-S4 and text). Again, as a racemic sample was used, an almost 50:50 ratio of  $S$ : $R$  is detected (282:273 events with  $|\cos(\theta)| > 0.6$ , see Fig. S5).

The technique still has several limitations: Volatile molecules and a large amount of substance are required due to the molecular beam source. Comparatively simple, rigid structures were studied. In the case of more complicated molecules, the kinematic properties of the fragments may not directly illustrate the geometric structure, making the identification of the abso-

lute configuration less straightforward. In this case, geometrical reconstruction or comparison with simple molecular dynamics simulations might become necessary, especially when several stereogenic elements are present. On a technical level, the probability of multi-fragment detection decreases dramatically with the amount of fragments, as both the fragmentation yield and the detection efficiency diminish exponentially with the number of fragments.

Stepwise fragmentation is a limitation as well. Additionally, when multi-ionization is slow compared to vibrational time scales, assignment can be hampered or even completely prohibited. For this purpose, faster ionization schemes with shorter laser pulses and higher laser intensity are required.

In conclusion, the present imaging approach allows for determination of absolute configuration of gas phase molecules on a per-molecule basis. Apart from a rigid structural model, it does not require theoretical input. Besides structure determination as demonstrated herein, the coincidence technique creates unique opportunities to study chirality in single molecules.

## References and Notes

1. R. Berger, *Relativistic Electronic Structure Theory, Part: 2, Applications*, P. Schwerdtfeger, ed. (Elsevier, Netherlands, 2004), pp. 188–288.
2. C. Daussy, *et al.*, *Phys. Rev. Lett.* **83**, 1554 (1999).
3. M. Quack, J. Stohner, M. Willeke, *Annu. Rev. Phys. Chem.* **59**, 741 (2008).
4. L. Pasteur, *Leçons de chimie professées en 1860 par MM. Pasteur, Cahours, Wurtz, Berthelot, Sainte-Claire Devile, Barral et Dumas* (Hachette, Paris, 1861), pp. 1–48.
5. J. H. van't Hoff, *Archives neerlandaises des sciences exactes et naturelles* **9**, 445 (1874).
6. J.-A. Le Bel, *Bull. Soc. Chim. Paris* **T22**, 337 (1874).

7. R. S. Cahn, C. Ingold, V. Prelog, *Angew. Chem. Int. Ed.* **5**, 385 (1966).
8. J. M. Bijvoet, A. F. Peerdeman, A. J. V. Bommel, *Nature* **168**, 271 (1951).
9. Z. Vager, R. Naaman, E. P. Kanter, *Science* **244**, 426 (1989).
10. T. Kitamura, T. Nishide, H. Shiromaru, Y. Achiba, N. Kobayashi, *J. Chem. Phys.* **115**, 5 (2001).
11. E. Fischer, *Ber. Dtsch. Chem. Ges.* **24**, 2683 (1891).
12. F. W. Lichtenthaler, *Angew. Chem. Int. Ed.* **31**, 1541 (1992).
13. Y. Inokuma, *et al.*, *Nature* **495**, 461 (2013).
14. A. D. Buckingham, *Chem. Phys. Lett.* **398**, 1 (2004).
15. R. Berger, *et al.*, *Angew. Chem. Int. Ed.* **51**, 8388 (2012).
16. C. Lux, *et al.*, *Angew. Chem. Int. Ed.* **51**, 5001 (2012).
17. D. Patterson, M. Schnell, J. M. Doyle, *Nature* **497**, 475 (2013).
18. J. Gagnon, K. F. Lee, D. M. Rayner, P. B. Corkum, V. R. Bhardwaj, *J. Phys. B* **41**, 215104 (2008).
19. B. Wales, *et al.*, *Nuclear Instruments and Methods in Physics Research A* **667**, 11-15 (2012).
20. J. Hine, A. M. Dowell, J. E. Singley, *J. Am. Chem. Soc.* **78**, 479 (1956).
21. J. Ullrich, *et al.*, *Rep. Prog. Phys.* **66**, 1463 (2003).
22. O. Jagutzki, *et al.*, *IEEE Transact. on Nucl. Science* **49**, 2477 (2002).

23. Further details on the measurement principle with six additional figures and four movies are available in the supporting material.
24. A. S. Alnaser, *et al.*, *Phys. Rev. A* **70**, 023413 (2004).

### **Acknowledgements**

The authors are indebted to David Avnir, Timur Isaev and Frieder Lichtenthaler for discussion. We acknowledge help by Moritz Meckel with some figures and support by Achim Czasch concerning data analysis. This work was supported by the State Initiative for the Development of Scientific and Economic Excellence (LOEWE) in the LOEWE-Focus ELCH. The momentum data used to draw the figures are provided in the SM. Raw data are archived at the University of Frankfurt (affiliation 1) and are available upon request.

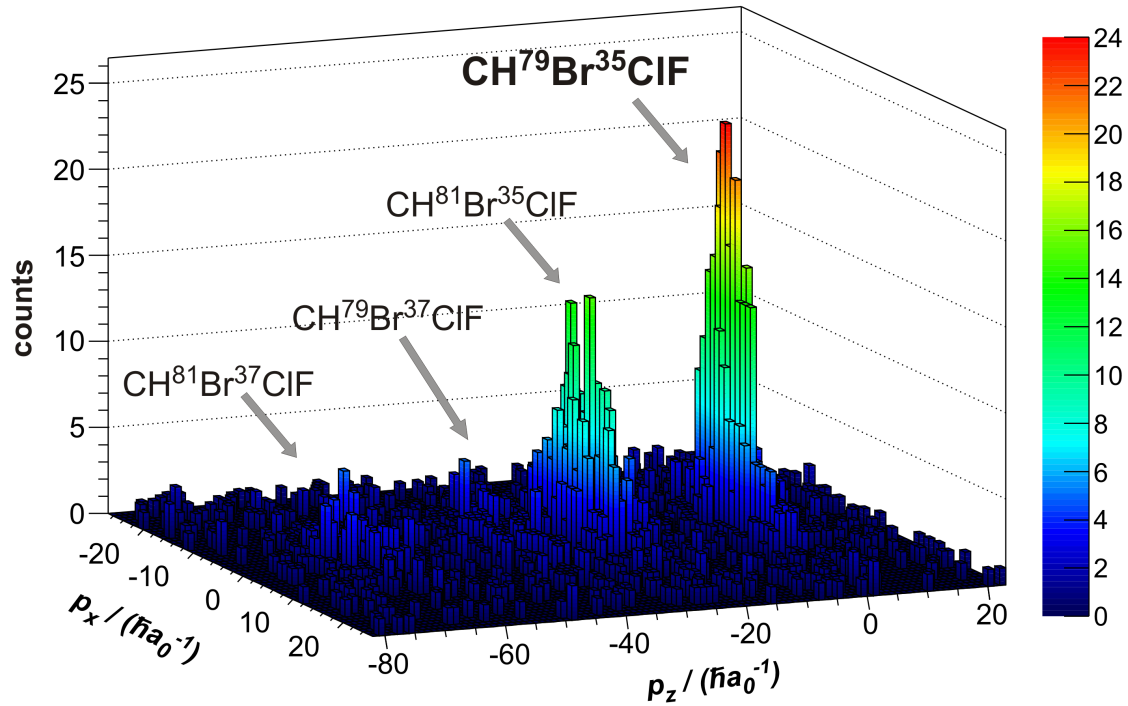


**Fig. 1.** Sum of linear momentum components in five-fold ionization of bromochlorofluoromethane, demonstrating the excellent resolution achieved in this experiment. Those events detected with  $p_x$  and  $p_z$  close to zero correspond to a fragment assignment to  $^{79}\text{Br}^+$ ,  $^{35}\text{Cl}^+$ ,  $^{19}\text{F}^+$ ,  $^{12}\text{C}^+$  and  $^1\text{H}^+$ . Fragments of other isotopologues can also be identified, but are not used in the present analysis. The atomic unit for momentum is defined as  $\hbar a_0^{-1} \approx 1.992 \cdot 10^{-24} \text{ kg m s}^{-1}$ .

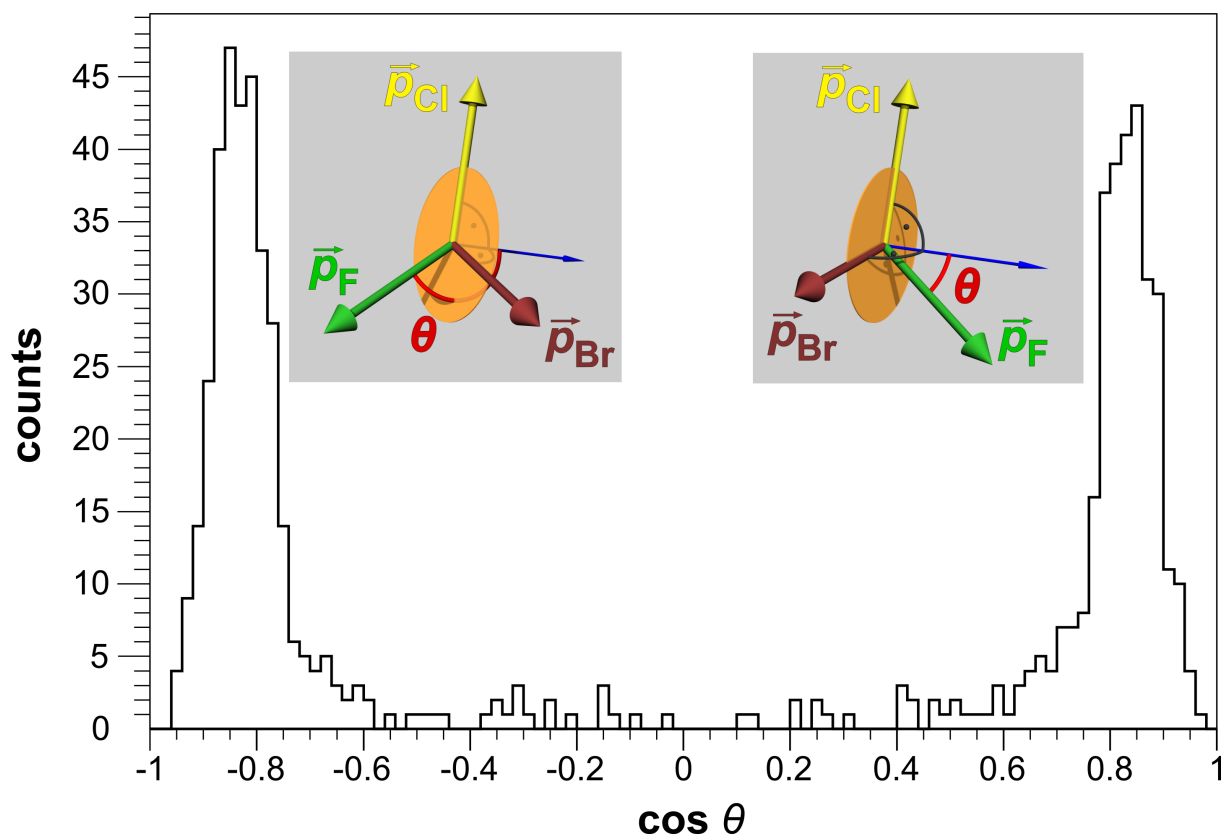


**Fig. 2.** Chiral discrimination for CHBrClF. The histogram for the cosine of the chirality angle  $\theta$  shows the clear separation between enantiomers in our racemic sample of CHBrClF. As is illustrated in the inset, the angle is defined via  $\cos(\theta) = \vec{p}_F \cdot (\vec{p}_{Cl} \times \vec{p}_{Br}) / (|\vec{p}_F| |\vec{p}_{Cl} \times \vec{p}_{Br}|)^{-1}$ . The peak at negative values of  $\cos(\theta)$  corresponds to the  $S$ -enantiomer, while the one at positive values corresponds to the  $R$ -enantiomer.

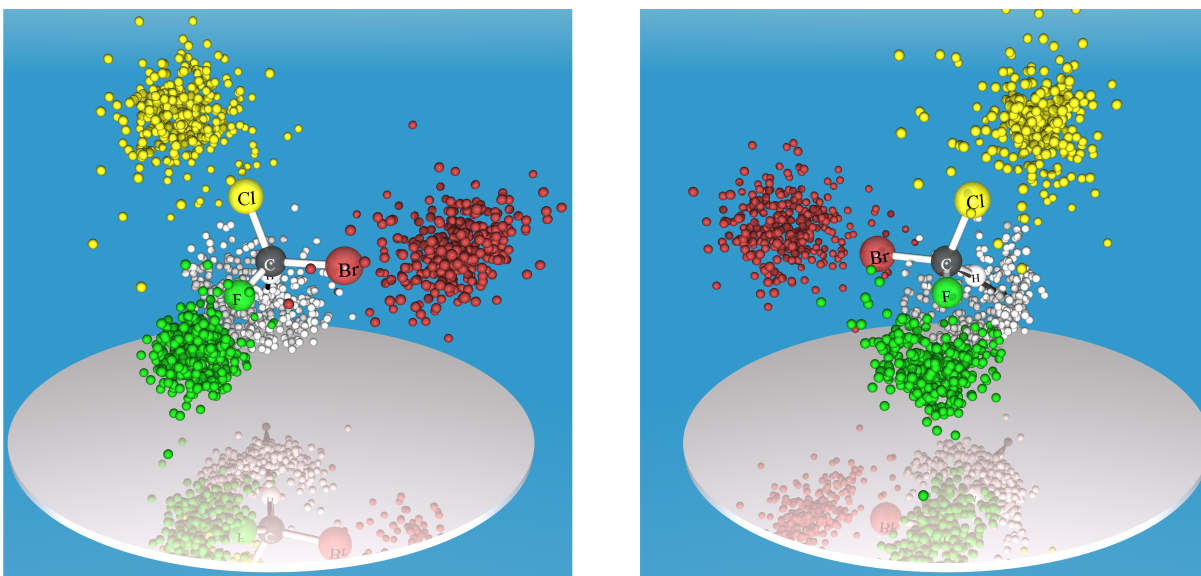


**Fig. 3.** Linear momenta in five-fold fragmentation of bromochlorofluoromethane enantiomers. Measured linear momenta in the five-fold fragmentation of (*S*)-CHBrClF (left,  $\cos(\theta) < -0.6$ ) and (*R*)-CHBrClF (right,  $\cos(\theta) > 0.6$ ) are indicated in the color codes C: black arrow, H: grey, F: green, Cl: yellow, Br: red. Momenta are rotated to the molecular frame of reference, defined by the momentum of the carbon ion and the momentum sum of bromine and chlorine ions. All momenta are normalized with respect to the carbon momentum. For better visibility, hydrogen momenta are expanded by a factor of 2. Whereas the substituents are expelled during the Coulomb explosion into the directions expected from the classical structural model, the central atom C is also accelerated away from the centre of mass and ejected in a similar direction as hydrogen. An animated version of the figure can be found in the SM (movies S1-S2).

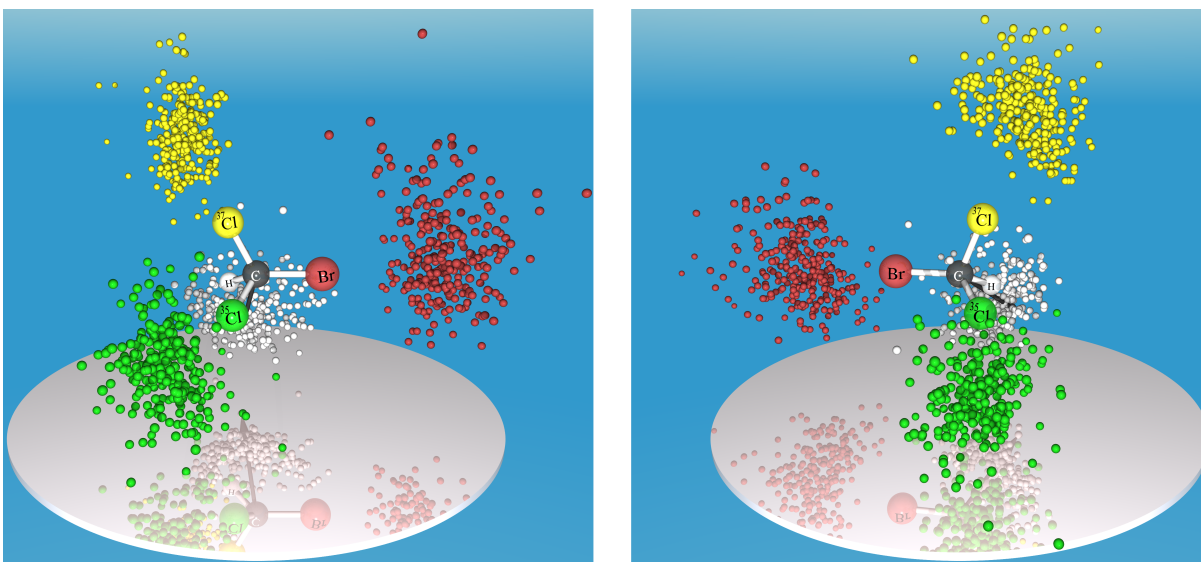


**Fig. 4.** Measured linear momenta in the five-fold fragmentation of (*S*)-CH<sup>79</sup>Br<sup>37</sup>Cl<sup>35</sup>Cl (left) and (*R*)-CH<sup>79</sup>Br<sup>37</sup>Cl<sup>35</sup>Cl (right). The color codes used correspond to C: black arrow, H: light grey, <sup>35</sup>Cl: green, <sup>37</sup>Cl: yellow, Br: red. Momenta are rotated to the molecular frame of reference, defined by the momentum of the carbon ion and the momentum sum of <sup>79</sup>Br and <sup>35</sup>Cl, and normalized with respect to the momentum of the carbon ion. Again, the hydrogen momentum is scaled by a factor of 2. Histogram and animated version of the figure can be found in the SM (Fig. S5, movies S3-S4). For a wider angle of vision, also a few outlier signals become clearly visible (Fig S7).

### **Supplementary content**

Description of the working principle of the coincidence experiment with two additional figures (S1 and S2), details on the measurement, details on the calibration, procedure for selecting break-ups in isotopically chiral systems with two additional figures (S3 and S4), histogram for  $\text{CH}^{79}\text{Br}^{37}\text{Cl}^{35}\text{Cl}$  break-ups, wider angle snapshots for figures 3 and 4 (S6 and S7), four movie files with animated versions of figures 3 and 4, two databases with the linear momentum data, Reference (24).